Chemical features of the photosensitizers new methylene blue N and S137 influence their subcellular localization and photoinactivation efficiency in *Candida albicans*

Gabriela Braga Rodrigues[a,§], Guilherme Thomaz Pereira Brancini[a,§], Sérgio Akira Uyemura[a], Luciano Bachmann[b], Mark Wainwright[c], Gilberto Ubida Leite Braga[a,*]

[a]Departamento de Análises Clínicas, Toxicológicas e Bromatológicas, Faculdade de Ciências Farmacêuticas de Ribeirão Preto, Universidade de São Paulo, Ribeirão Preto, SP 14040-903, Brazil

[b]Departamento de Física, Faculdade de Filosofia, Ciências e Letras de Ribeirão Preto. Universidade de São Paulo, Ribeirão Preto, SP 14040-903, Brazil

[c]School of Pharmacy and Biomolecular Sciences, Liverpool John Moores University, Liverpool L3 3AF, United Kingdom

*Corresponding author: Faculdade de Ciências Farmacêuticas de Ribeirão Preto, Universidade de São Paulo, Ribeirão Preto, São Paulo, 14040-903, Brazil.

E-mail adress: gbraga@fcfrp.usp.br.

[§]These authors contributed equally to this work.

ABSTRACT

Antimicrobial photodynamic treatment (APDT) has emerged as an effective therapy against pathogenic fungi with both acquired and intrinsic resistance to commonly used antifungal agents. Success of APDT depends on the availability of effective photosensitizers capable of acting on different fungal structures and species. Among the phenothiazinium dyes tested as photoantifungals, new methylene blue N (NMBN) and the novel pentacyclic compound S137 are the most efficient. In the present study we compared the effects of APDT with NMBN and S137 on the survival of *Candida albicans* and employed a set of fluorescent probes (propidium iodide, FUN-1, JC-1, DHR-123 and DHE) together with confocal microscopy and flow cytometry to evaluate the effects of these two chemically diverse photosensitizers on cell membrane permeability, metabolism and redox status, and mitochondrial activity. Taken together, our results indicate that, due to chemical features resulting in different lipophilicity, NMBN and S137 localize to distinct subcellular structures and hence inactivate *C. albicans* cells via different mechanisms. S137 localizes mostly to the cell membrane and, upon light exposure, photo-oxidizes membrane lipids. NMBN readily localizes to mitochondria and exerts its photodynamic effects there, which was observed to be a less effective way to achieve cell death at lower light fluences.

Keywords: antimicrobial photodynamic treatment, fungal photodynamic inactivation, phenothiazine photosensitizers, fluorescent probes, reactive oxygen species

1. Introduction

Several procedures in modern medicine, such as solid organ and hematopoietic stem cell transplantations, surgeries, autoimmune disease therapies, and uncontrolled HIV infection make millions of patients vulnerable to lethal fungal diseases (Köhler et al. 2015; Limper et al. 2017). *Candida albicans*, usually a harmless commensal fungus, is also an opportunistic pathogen for immunocompromised people and the major human fungal pathogen in the USA and several other countries (Nishimoto et al. 2020). Today, fungal infections are among the most difficult diseases to treat in humans (Köhler et al. 2015). One of the factors that makes treatment so difficult is the rapid acquisition of resistance to all of the only four major classes of antifungal agents clinically available: azoles, polyenes, echinocandins, and a nucleotide analog (Chang et al. 2019; Perlin et al. 2017; Shor and Perlin 2015). Additionally, many species of *Candida*, such as *Candida auris* and *Candida glabrata* are intrinsically resistant to some antifungal classes (Chang et al. 2019; Nishimoto et al. 2020; Rhodes and Fisher 2019). Multidrug resistance can eliminate treatment options completely, which has a serious effect on patient survival (Perlin et al. 2017).

The emergence of resistance to currently used antifungals has promoted the development of novel antifungal approaches, such as ~~the~~ antimicrobial photodynamic treatment (APDT). The basic principle behind photodynamic antimicrobial inactivation is the combination three factors: (1) visible or near-infrared light, (2) molecular oxygen, and (3) a photosensitizer (PS). Light exposure excites the photosensitizer to a singlet state. Then, intersystem crossing results in a photosensitizer in an excited triplet state which can interact with molecular oxygen either via electron or energy transfer. Electron transfer, also called Type I reaction~~s~~, usually result<u>s</u> in the formation of radicals such as <u>the</u> superoxide radical anion. Conversely, energy transfer or Type II reaction results in

the formation of singlet oxygen. In either case, reactive oxygen species (ROS) such as singlet oxygen, superoxide radical anions, and hydroxyl radicals have a broad spectrum of activity and can damage several microbial targets ~~such as~~as among the various proteins, lipids, and nucleic acids encountered, therefore making selection of resistant strains unlikely (Brancini et al. 2016; Wainwright et al. 2017). Among photoantimicrobials evaluated as antifungals, the phenothiazinium dyes methylene blue and toluidine blue are the most commonly used, mainly due to their low toxicity and their long-established use for other clinical applications (Rodrigues et al. 2013; Wainwright et al. 2017). Phenothiazinium derivatives with improved photoantimicrobial activity against yeasts and filamentous fungi such as new methylene blue N (NMBN) and the novel pentacyclic compound S137, have been identified (Dai et al. 2011; Rodrigues et al. 2013). APDT with NMBN and S137 has been shown to be highly effective against fungi of the genera *Aspergillus* (de Menezes et al. 2014), *Candida* (Dai et al. 2011; Rodrigues et al. 2013), *Colletotrichum* (de Menezes et al. 2014), *Neoscytalidium* (Tonani et al. 2018), and *Trichophyton* (Rodrigues et al. 2012).

The most important factor determining the outcome of APDT is how a photosensitizer interacts with cells of the target microorganism, with its subcellular localization being of particular interest (Gonzales et al. 2017; de Menezes et al. 2014; de Menezes et al. 2016). This is because ROS have a short half-life and therefore exert their action in the vicinity of their production site (Castano et al. 2004). Cellular uptake and intracellular localization is determined by chemical and structural features of the PS (e.g. molecular mass, lipophilicity, charge distribution, number of H-bond donors and acceptors, etc.), the concentration of the PS, the incubation time, and the phenotypic characteristics of the target cells (Castano et al. 2004). PS characteristics such as charge

type and distribution as well as lipophilicity may be controlled by informed synthesis (Wainwright and Giddens 2003).

The use of confocal laser scanning fluorescence microscopy has made the determination of intracellular localization of PS much easier. Colocalization of subcellular organelle-specific fluorescent probes with differing fluorescence emission peak to that of the PS can be used to more closely identify the site of localization and these probes can also be used to identify sites of damage after illumination (Castano et al. 2004).

The photosensitizers NMBN and S137 are chemically and structurally distinct, and consequentially present different outcomes when used in APDT. For instance, use of S137 usually results in cell damage even in the dark (dark toxicity) and its microbial photoinactivation tends to be higher at lower light fluences when compared to NMBN. As previously mentioned, PS subcellular localization can greatly influence the results of APDT. Therefore, here we compared NMBN and S137 by employing a set of fluorescent probes (propidium iodide, FUN-1, JC-1, DHR-123, and DHE) together with confocal microscopy and flow cytometry in order to evaluate potential PS subcellular localization as well as the mechanism behind APDT with these PS.

2. Materials and Methods

2.1. C. albicans strain and growth conditions

C. albicans strain ATCC 64548 was obtained from the American Type Culture Collection (ATCC) (Manassas, USA). Cells were grown on Sabouraud Dextrose Agar (SDA) medium (BD Difco, USA) in the dark, at 35 °C, for 48 h. Cells from isolated colonies were transferred to 150-mL Erlenmeyer flasks containing 50 mL of YPD medium [1% Yeast Extract (BD Difco, Sparks, USA), 2% Peptone (BD Difco) and 2%

Dextrose (Vetec, Duque de Caxias, Brazil)]. Cultures were incubated in the dark at 35 °C for 6 h under shaking (100 rpm). Cells were then washed in phosphate-buffered saline (PBS, pH 7.4) (8,000 × *g*, 5 min) and cell concentration was adjusted by counting in a hemocytometer and performing the appropriate dilutions in PBS.

2.2. Photosensitizers

New Methylene Blue N zinc chloride double salt (NMBN) was purchased from Sigma-Aldrich (catalog number 202096; St. Louis, USA) (Fig. 1A). The pentacyclic phenothiazinium photosensitizer S137 was synthesized as previously described (Wainwright et al. 2011) (Fig. 1A). Stock solutions of the PS were prepared in water at a concentration (500 µM) two hundred-fold greater than the concentration used in the study. The solutions were stored in the dark at −20 °C for up to 2 weeks. Dilutions were prepared in PBS. Absorption spectra of the PS were obtained with a Ultrospec™ 2100 Pro UV-visible spectrophotometer (GE Healthcare) in water (Fig. 1B).

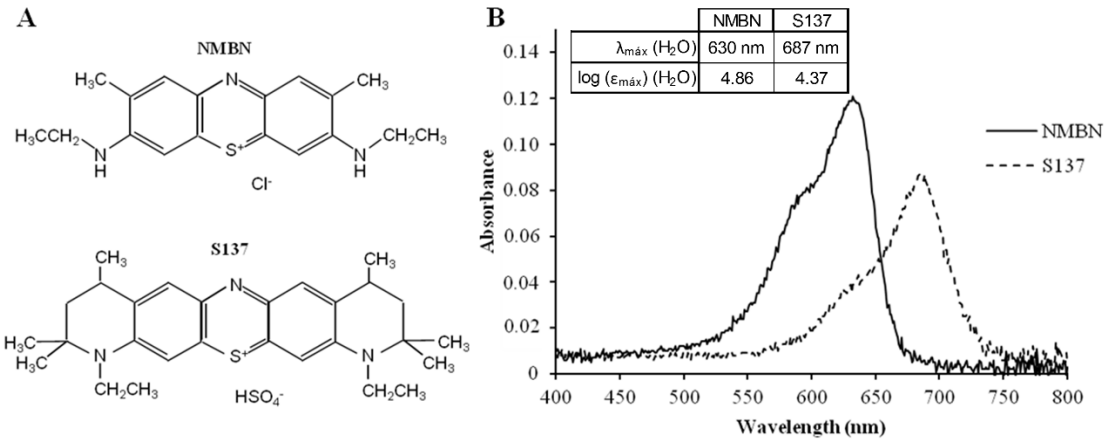

Fig. 1. Chemical structure (**A**) and absorption spectra (**B**) of the photosensitizers NMBN and S137

2.3. Light exposure

Light was provided by an array of 96 light-emitting diodes (LED) with peak emission at 631 ± 20 nm and an irradiance of 13.89 mW cm^{-2}. Irradiance and emission spectrum (Fig. 2) were obtained with a USB spectroradiometer (Ocean Optics, Dunedin, USA) as previously described (Rodrigues et al. 2012).

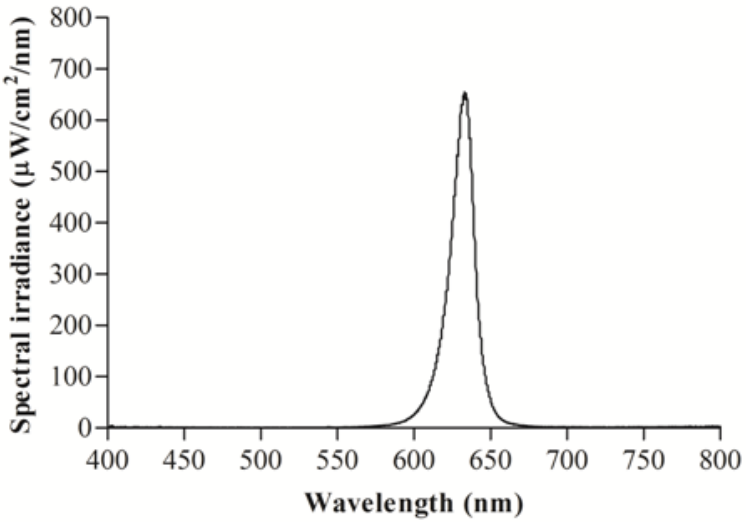

Fig. 1. Irradiance spectrum of the red light source used in this study

2.4. Photodynamic treatment

Five mL of the fungal cell suspension and 5 mL of the PS (NMBN or S137) were added to 15 mL tubes (TPP, Switzerland). Final concentrations of cells and PS in the mixture were 2×10^7 cells mL^{-1} and 2.5 µM of NMBN or S137. Tubes were kept in the dark for 30 min at 28 °C and light exposure was performed under agitation in a 60-mm Petri dish. The fluences used were 3, 9, and 14 J cm^{-2} (obtained after 3.42, 10.28, and 17.13 min, respectively). Relative cell survival after APDT was evaluated for each fluence used by counting colony-forming units (CFU). To do this, the initial suspensions were serially diluted tenfold in PBS to give dilutions of 10^{-1} to 10^{-3}. Fifty microliters were then spread on the surface of 5 mL of SDA medium in Petri dishes (60 × 15 mm). Three

157 replicate-dishes were prepared for each light treatment. The dishes were incubated in the
158 dark at 35 °C. After 24 h, CFU were counted at 8× magnification daily for up to 4 days.
159 A dark control group was obtained by treating cells with PS but never exposing them to
160 light. A light control group was prepared by exposing cells alone (in the absence of PS)
161 to light fluences of 3, 9, and 14 J cm^{-2}. Absolute controls consisted of cells unexposed to
162 either light or PS. Relative survival was calculated as the ratio of CFU of fungal cells
163 treated only with light (light effect), only with PS (toxicity in the dark), and light and PS
164 (APDT) to CFU treated with neither light nor PS. Three independent experiments were
165 performed.
166
167 *2.5. Propidium iodide (PI) staining and visualization*
168 After APDT with NMBN or S137, cell suspensions were washed with PBS to
169 remove excess PS. Cells were then suspended in a 1.5 µM PI (Sigma-Aldrich, catalog
170 number P4170) solution prepared in PBS immediately before being used. Flow cytometry
171 was performed in a BD FACSCanto I equipment and BD FACSDiva software. In each
172 experiment, ten thousand events were monitored with excitation at 488 nm and detection
173 between 564 and 606 nm. Cells not treated with PS and cells treated with 70% ethanol
174 were used as negative and positive controls, respectively. Three independent experiments
175 were performed.
176 Confocal fluorescence microscopy was used to visualize PI entry into cells. After
177 APDT and PI staining, cells were centrifuged (10,000 × *g*, 2 min) and the supernatant was
178 discarded. Three microliters of 2% Ultra Pure low-melting-point agarose (Invitrogen) and
179 3 µL of Fluoromount (Sigma) were added to 3 µL of cell pellet and the mixture was used
180 to mount the slide. Confocal microscopy was performed on a Leica DMI 6000 CS,
181 scanner TCS SP8 with a 63× objective lens (f/1.4) and using oil immersion. For PI

visualization, excitation was performed with an Optically Pumped Semiconductor Laser at 488 nm and detection at 597-637 nm.

2.6. FUN-1 staining and visualization

After APDT with NMBN or S137, cells were washed with 10 mM HEPES pH 7.2 (Sigma-Aldrich) supplemented with 2% glucose (hereinafter referred to as GH buffer) to remove excess PS. Cells were then suspended in a 0.5 µM FUN-1 solution (Molecular Probes, Life Technologies, Eugene, OR, USA) prepared in GH buffer. Cells were incubated in the dark under shaking (300 rpm) at 30 °C for 30 min. The spectrofluorimetric analysis was performed in black 96-well plates with a Synergy 2 equipment (BioTek®, Winooski, USA). Excitation was set to 475-495 nm and detection to 518-538 nm (green fluorescence) and 580-600 nm (red fluorescence). Three independent experiments were performed.

For confocal microscopy, FUN-1-stained cells were centrifuged (10,000 × *g*, 2 min) and slides were mounted and visualized as described above for PI. Laser excitation was set to 488 nm and detection to 530-560 nm (green fluorescence) and 604-636 nm (red fluorescence).

2.7. JC-1 staining and visualization

After APDT with NMBN and S137, cells were washed (10,000 × *g*, 2 min) with GH buffer to remove excess PS. Cells were then suspended in a 5 µM JC-1 (Molecular Probes, Life Technologies, USA) solution prepared in GH buffer and incubated in the dark under shaking (300 rpm) at 35 °C for 30 min. Then, cells were washed twice with GH buffer and flow cytometry was performed as described previously. A total of 10,000 events were monitored. Excitation was set to 488 nm and detection to 515-545 nm (green

fluorescence) and 564-606 nm (red fluorescence). Three independent experiments were performed.

Confocal microscopy was performed as described previously. Laser excitation was set to 488 nm and detection to 505-550 nm (green fluorescence) and 575-630 (red fluorescence).

2.8. Dihydrorhodamine-123 (DHR-123) staining and visualization

After APDT with NMBN or S137, cells were washed (10,000 × *g*, 2 min) with GH buffer to remove excess PS. Cells were then suspended in a 5 μg mL^{-1} DHR-123 solution (Sigma-Aldrich, catalog number D1054) prepared in GH buffer and incubated in the dark at 25 °C for 120 min. Flow cytometry was performed as described previously. A total of 10,000 events were monitored. Excitation was set to 488 nm and detection to 515-545 nm. Three independent experiments were performed.

Confocal microscopy was performed as described previously. Laser excitation was set to 488 nm and detection to 501-570 nm.

2.9. Dihydroethidium (DHE) staining and visualization

After APDT with NMBN or S137, cells were washed (10,000 × *g*, 2 min) with GH buffer to remove excess PS. Cells were then suspended in a 20 μM DHE (Sigma-Aldrich, catalog number D7008) solution prepared in GH buffer and incubated in the dark at 25 °C for 45 min. Flow cytometry was performed in a Guava EasyCyte 8HT (Merck Millipore, Darmstadt, Germany). In each experiment, a total of 30,000 events were analyzed using the red filter. Three independent experiments were performed.

Confocal microscopy was performed as described previously. Laser excitation was set to 552 nm and detection to 556-624 nm.

232

233 *2.10. PS lipophilicity prediction*

234 Lipophilicity of NMBN and S137 (as expressed by logD as a function of pH) was
235 calculated with the MarvinJS logD Predictor software (ChemAxon). PS structures used
236 in the predictions are those depicted in Fig. 1.

237

238 *2.11. Statistical analysis*

239 Differences between means were analyzed via ANOVA with Tukey's post-test.
240 Significance threshold was set to $P < 0.05$. Statistical analyses were performed with SAS®
241 9.2 software (SAS Analytics, USA).

242

243 **3. Results**

244 *3.1. C. albicans survival after APDT*

245 The PS NMBN and S137 were compared in terms of cell mortality after APDT
246 with fluences of 3, 9, and 14 J cm^{-2}. Importantly, treatment with PS alone or light exposure
247 alone did not result in cell mortality (Fig. 3). At 3 J cm^{-2}, S137 was a much more effective
248 PS, reducing cell viability by 99.98% (3.70 log_{10}) whereas NMBN achieved only 85.2%
249 (0.83 log_{10}) under the same conditions (Fig. 3). Increasing fluence to 9 and to 14 J cm^{-2}
250 allowed NMBN and S137 to achieve similar cell mortality, which was above four orders
251 of magnitude for both PS (Fig. 3).

252

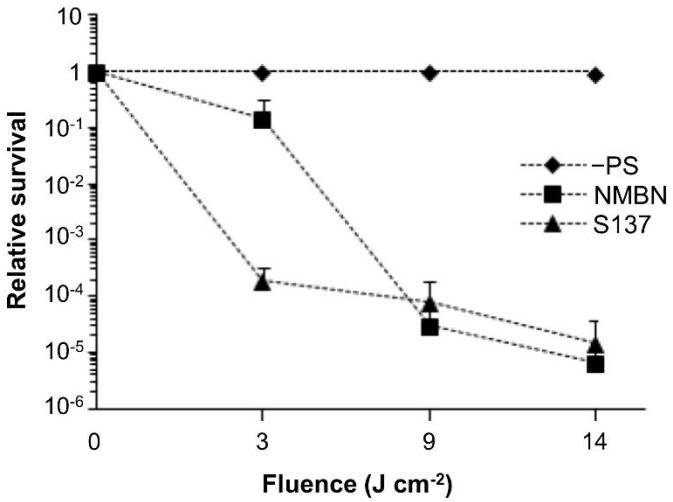

Fig. 3. Relative survival of *Candida albicans* after antimicrobial photodynamic treatment with NMBN and S137 as a function of light fluence. Control groups were either treated with light alone (-PS) or photosensitizer alone (fluence = 0 J cm^{-2}). Error bars are the standard deviation from three independent experiments.

3.2. Propidium iodide staining and visualization

Staining with PI was used to study fungal membrane disturbance caused by the PS both in the dark and after APDT. In the dark, NMBN caused little to no PI labeling as evaluated by flow cytometry whereas S137 caused about 80% of cells to become PI-positive (Fig. 4). The percentage of PI-positive cells achieved 100% for S137 already at the lowest fluence used (3 J cm^{-2}) whereas this number was only about 40% for NMBN even at the highest fluence (14 J cm^{-2}) (Fig. 4).

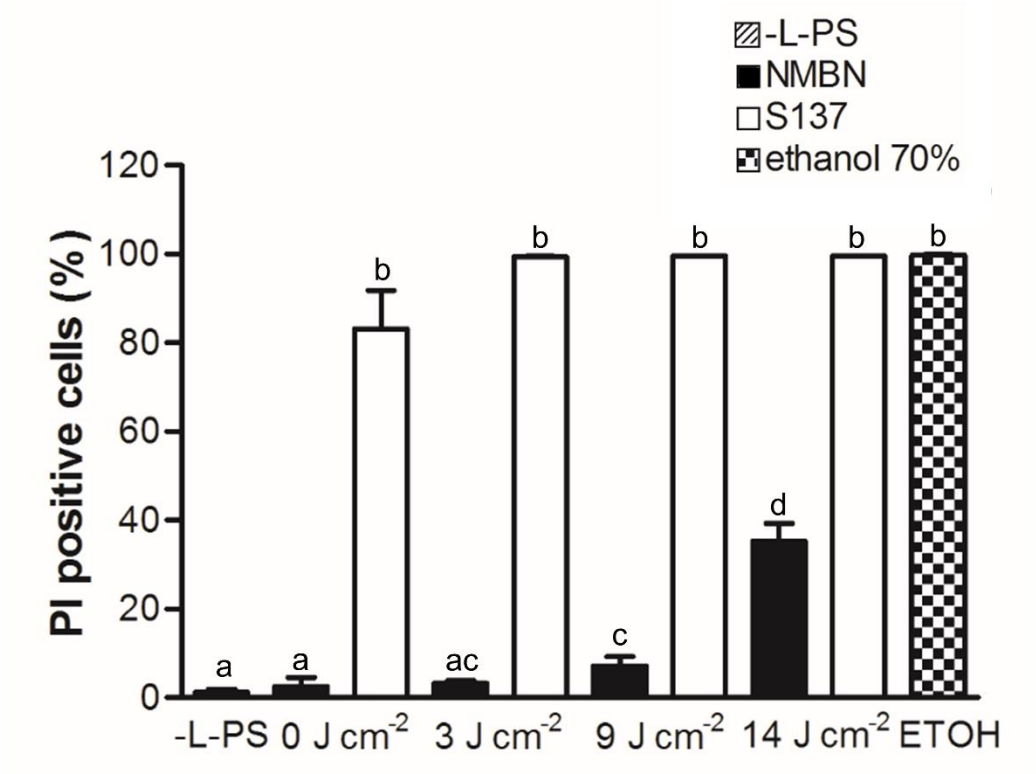

Fig. 4. *Candida albicans* Propidium iodide staining as evaluated by flow cytometry. Cells were treated with either NMBN or S137 and control groups received neither light nor photosensitizer (-L -PS). Different lower case letters indicate that means are statistically different. Error bars are the standard deviation from three independent experiments.

Although adding S137 resulted in PI permeability already in the dark in flow cytometry experiments, confocal fluorescence microscopy could not distinguish between NMBN and S137 in the dark (Fig. 5). At 14 J cm^{-2}, both NMBN- and S137-treated cells were stained (Fig. 5).

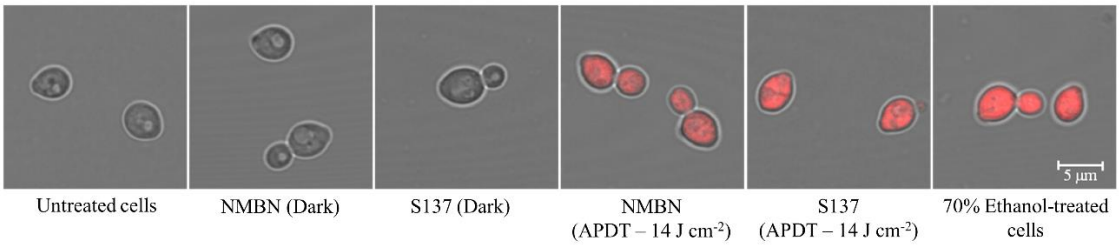

Fig. 5. *Candida albicans* propidium iodide staining as evaluated by confocal fluorescence microscopy. Control cells were not treated with either photosensitizer or light. NMBN

and S137 were used either in the dark or under light at a fluence of 14 J cm^{-2}. Images are representative of three independent experiments.

3.3. FUN-1 staining and visualization

FUN-1 is a dye that diffuses inside fungal cells and stains them green irrespective of viability. However, in viable cells, further processing of the dye results in the appearance of red fluorescent spots accompanied by reduced green fluorescence. Therefore, the red/green fluorescence ratio is used as a marker of cell viability in flow cytometry experiments. Cells treated with either NMBN or S137 in the dark were not significantly different from untreated cells (Fig. 6). After APDT, the red/green fluorescence ratio decreased proportionally with increasing fluences and both PS were similar in this regard, although the majority of differences were not statistically significant (Fig. 6).

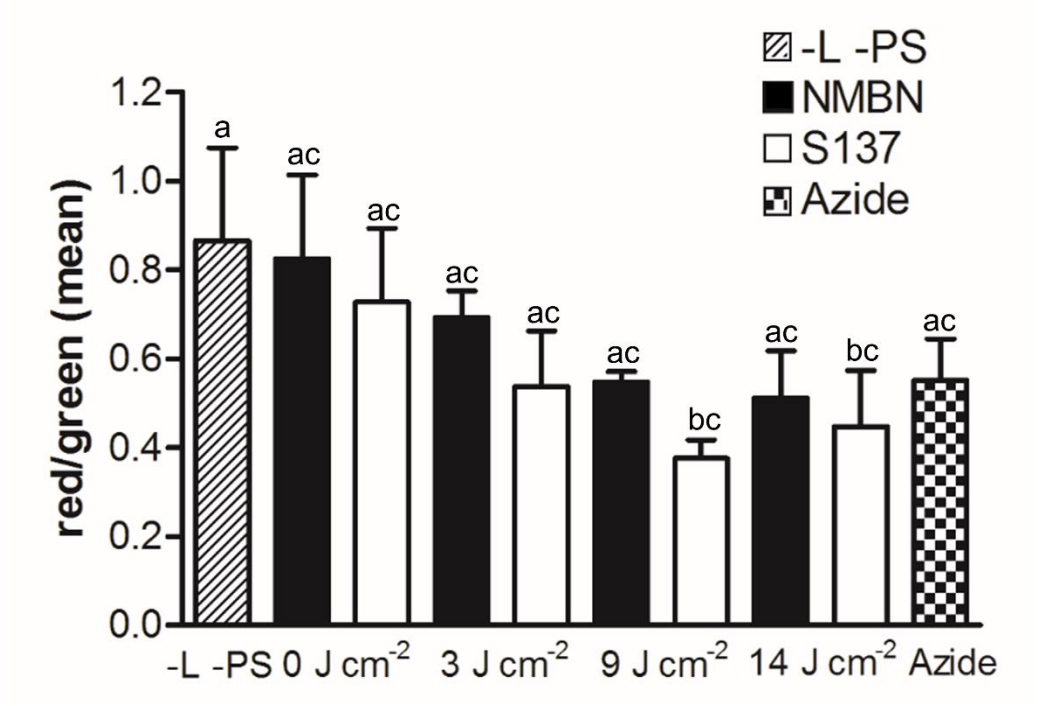

Fig. 6. *Candida albicans* FUN-1 staining as evaluated by spectrofluorimetry. Cells were treated with either NMBN or S137 and control groups received neither light nor

297 photosensitizer (-L -PS). Different lower case letters indicate that means are statistically
298 different. Error bars are the standard deviation from three independent experiments.

299

300 As expected, confocal fluorescence microscopy showed the accumulation of
301 vacuolar-like red fluorescence in untreated cells and those that were treated with either
302 PS in the dark, indicating normal viability (Fig. S1). After APDT with 14 J cm^{-2}, these
303 red spots were lost and cells stained yellow (Fig. S1).

304

305 *3.4. JC-1 staining and visualization*

306 JC-1 is a dye that accumulates in mitochondria in a membrane potential-dependent
307 manner. This accumulation is indicated by a red-to-green fluorescence shift. The loss of
308 mitochondrial membrane potential (depolarization) reduces the red/green fluorescence
309 ratio. Treating cells with S137 in the dark resulted in no mitochondria depolarization.
310 However, NMBN caused considerable loss of membrane potential in the dark (Fig. 7).

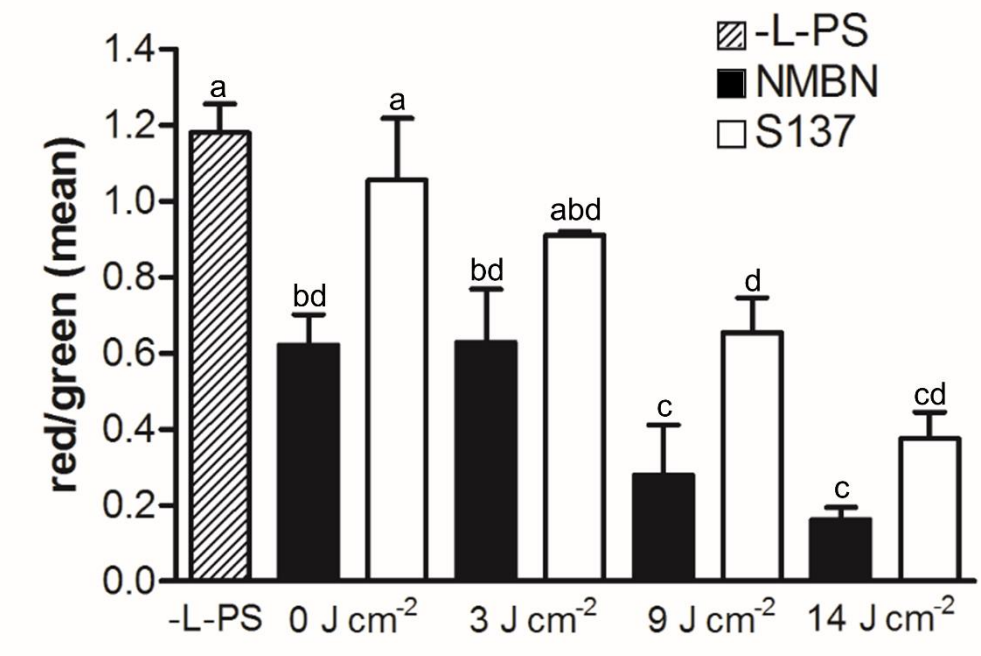

311

312 **Fig. 7.** *Candida albicans* JC-1 staining as evaluated by flow cytometry. Cells were treated
313 with either NMBN or S137 and control groups received neither light nor photosensitizer
314 (-L -PS). Different lower case letters indicate that means are statistically different. Error
315 bars are the standard deviation from three independent experiments

316

317 Mitochondrial membrane potential decreased upon light exposure for both PS,
318 even though S137 required a fluence of 9 J cm^{-2} to achieve a statistically significant
319 difference from the control (Fig. 7).

320 Although flow cytometry experiments showed that NMBN can reduce
321 mitochondrial membrane potential already in the dark, fluorescence microscopy did not
322 indicate the same result as both NMBN and S137, when used in the dark, were very
323 similar to untreated cells (Fig. S2). Upon light exposure (14 J cm^{-2}), the expected decrease
324 in red/green fluorescence ratio was observed for both PS. However, loss of red
325 fluorescence was higher for NMBN when compared to S137 (Fig. S2), which reflects
326 flow cytometry experimental data (Fig. 7).

327

328 *3.5. Dihydrorhodamine-123 (DHR-123) staining and visualization*

329 DHR-123 is an uncharged and membrane-permeant compound that, upon
330 oxidation, is converted to the mitochondrial dye rhodamine-123, emitting green
331 fluorescence. Treating cells with either PS in the dark did not result in a significant
332 increase in green fluorescence. Light exposure at a fluence of 3 J cm^{-2} revealed that S137
333 generated more DHR-123-oxidizing species than did NMBN (Fig. 8), which was also
334 observed for the fluence of 9 J cm^{-2}. At 14 J cm^{-2}, both PS leveled off and produced about
335 the same amount of oxidizing species (Fig. 8).

336

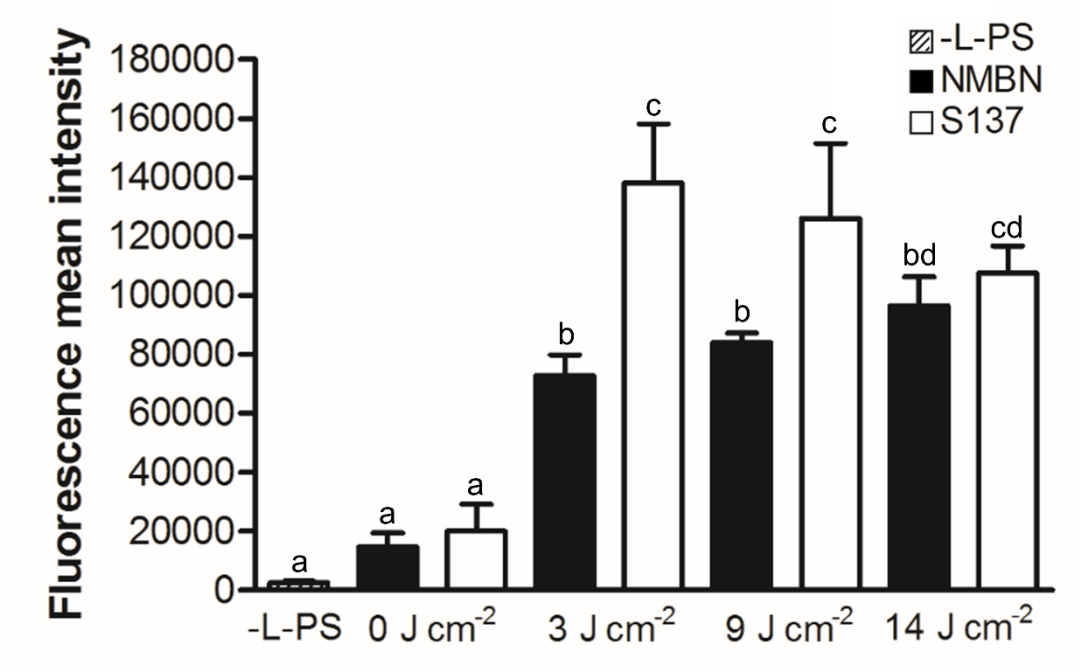

Fig. 8. *Candida albicans* Dihydrorhodamine-123 staining as evaluated by flow cytometry. *Candida albicans* cells were treated with either NMBN or S137 and control groups received neither light nor photosensitizer (-L -PS). Different lower case letters indicate that means are statistically different. Error bars are the standard deviation from three independent experiments.

Fluorescence microscopy, as expected, showed no green fluorescence in untreated cells and cells treated with either PS (Fig. S3). Strong green fluorescent emission was observed at 14 J cm^{-2}, which was similar for NMBN and S137 (Fig. S3).

3.6. Dihydroethidium (DHE) staining and visualization

DHE is widely regarded as an indicator of superoxide anion radical ($O_2^{\bullet-}$) production because DHE oxidation by $O_2^{\bullet-}$ gives 2-hydroxyethidium, which emits red fluorescence. However, unspecific oxidation of DHE by other ROS results in ethidium, which also emits red fluorescence and is hard to distinguish from 2-hydroxyethidium. Therefore, we employed DHE as a general indicator of ROS and not specifically of $O_2^{\bullet-}$. Neither NMBN nor S137 leads to ROS production in the dark when compared to

untreated cells (Fig. 9). ROS production increased upon light exposure, although we observed no difference between NMBN and S137 (Fig. 9).

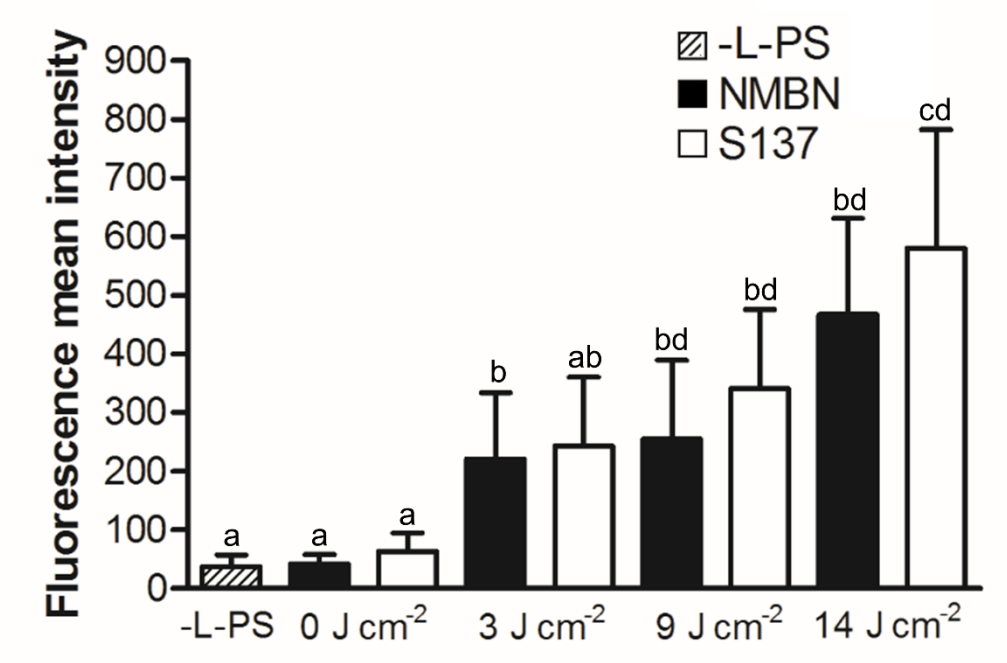

Fig. 9. *Candida albicans* dihydroethidium staining as evaluated by flow cytometry. Cells were treated with either NMBN or S137 and control groups received neither light nor photosensitizer (-L -PS). Different lower case letters indicate that means are statistically different. Error bars are the standard deviation from three independent experiments.

Confocal fluorescence microscopy reflected flow cytometry results: no red fluorescence was observed in the dark for either PS and red fluorescence was observed at 14 J cm^{-2} that was indistinguishable between NMBN and S137 (Fig. S4).

3.7. NMBN and S137 lipophilicity prediction

In the dark, S137 caused extensive membrane damage (Fig. 4) and NMBN reduced mitochondrial membrane potential (Fig. 7). These observations prompted an investigation of PS lipophilicity. Predicting logD as a function of pH for both PS revealed that whereas NMBN is of moderate lipophilicity (logD = 3.08 at pH 7), S137 is highly

373 lipophilic (logD = 6.26) (Fig. 10A). For comparison, we also calculated logD values for
374 the membrane component ergosterol (logD = 6.63) and the mitochondria-specific dye
375 MitoTracker™ Red CMXRos (logD = 2.72) (Fig. 10B).
376

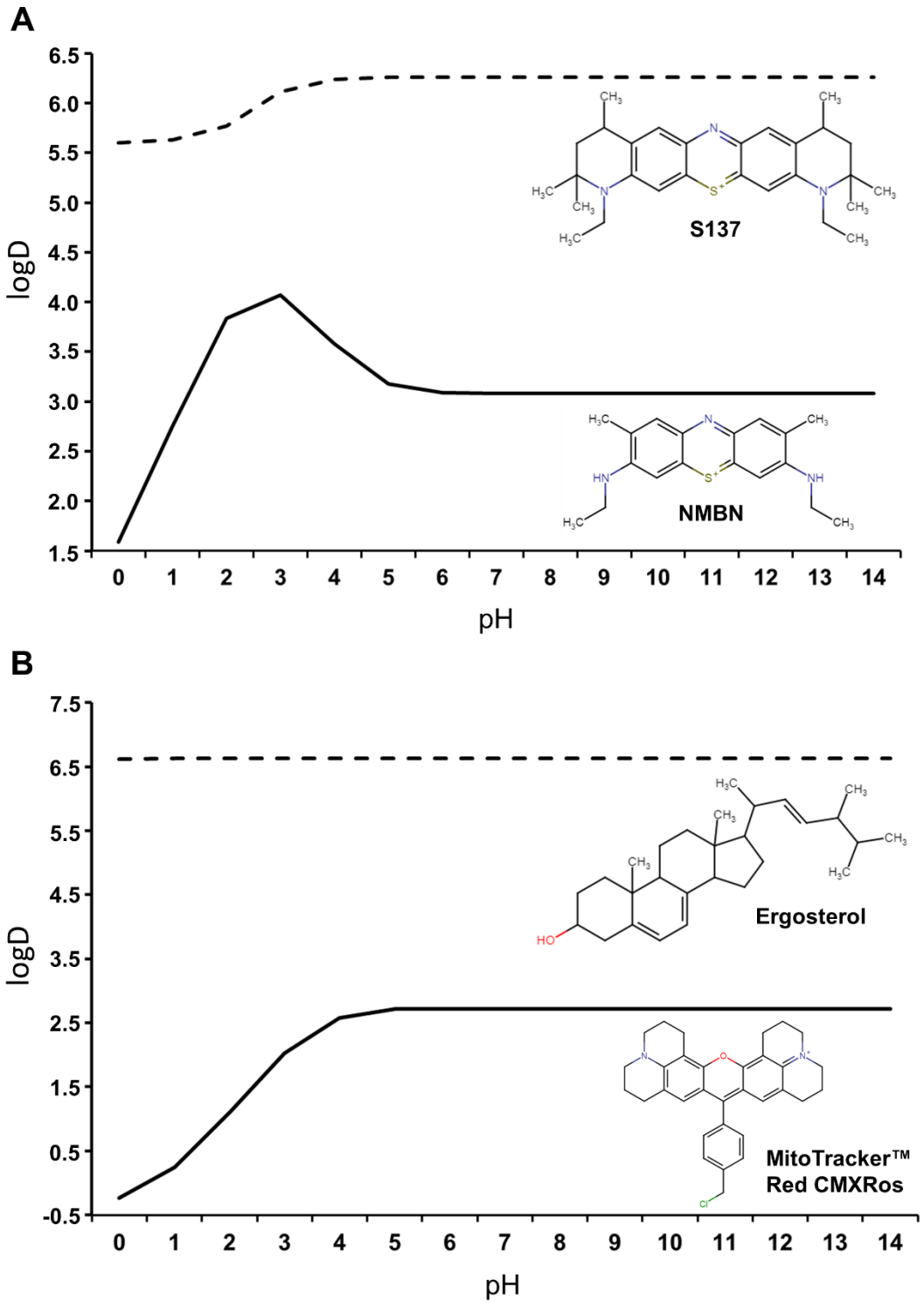

Fig. 10. Prediction of lipophilicity (logD) as a function of pH for the photosensitizers NMBN and S137 (**A**), and membrane-associated ergosterol and mitochondrial dye MitoTracker™ Red CMXRos (**B**).

4. Discussion

Understanding the mechanism behind microbial photoinactivation with different PS is a key step in improving the efficiency of APDT and in selecting the most appropriate PS based on target microorganism and condition. APDT of *C. albicans* with the PS NMBN and S137 revealed that the latter achieves increased cell mortality at lower fluences when compared to the former (Fig. 3). Under the experimental conditions used here, NMBN is expected to produce more singlet oxygen compared to S137 as its peak absorption (630 nm, Fig. 1B) essentially matches that of the light system used (631 nm). Furthermore, NMBN has a higher molar absorption coefficient (Fig. 1B). Indeed, recent observations from our group have shown that singlet oxygen quantum yield of NMBN is higher than that of S137 (De Menezes et al., in preparation). Therefore, the different efficiency in APDT between NMBN and S137 at 3 J cm^{-2} cannot be explained by photophysical properties alone. To better understand this phenomenon, we employed a set of fluorescent dyes analyzed by both flow cytometry (or spectrofluorimetry in the case of FUN-1) and confocal fluorescence microscopy.

Initially, we used FUN-1 and PI as vital dyes. FUN-1 was not capable of distinguishing the difference between APDT with NMBN and S137 at 3 J cm^{-2} (Fig. 6), showing that it is not an adequate dye to evaluate cell mortality after APDT. Results obtained with PI showed that S137 caused extensive membrane permeabilization even in the dark whereas NMBN could only permeabilize the membrane at higher light fluences (Fig. 4). Interestingly, membrane permeabilization by S137 was unrelated to cell survival as this PS caused no mortality in the dark (Fig. 3). This is in agreement with prior works showing that membranes of stressed yeast and conidia of filamentous fungi can become permeable to PI without loss of cell viability (Davey and Hexley 2011; de Menezes et al. 2016; Tonani et al. 2018).

The above-mentioned increase in PI permeability after S137 treatment in the dark was easily quantified by flow cytometry (Fig. 4) but was not observed by confocal fluorescence microscopy (Fig. 5). This discrepancy between the two techniques is likely a consequence of differences in sensitivity. Flow cytometry is more sensitive than confocal microscopy because, in the latter, out-of-focus image signals are ignored by the confocal system, rendering this technique inadequate for faint fluorescence probes (Basiji et al. 2007). On the other hand, flow cytometry sacrifices all imaging capabilities in favor of greater sensitivity. In fact, flow cytometry can detect as few as 100 fluorescent molecules per cell (Basiji et al. 2007), making it the method of choice for quantitative measurement of a heterogeneous population of cells. Therefore, we can hypothesize that confocal microscopy could not detect the difference between NMBN and S137 in the dark for PI because the number of PI molecules entering the cell in S137-treated samples is insufficient to produce a fluorescence signal that is strong enough to be detected by confocal microscopy. Further evidence of this difference in sensitivity is that for other fluorescent probes (such as DHR-123) confocal microscopy fails to detect any fluorescent signal for both PS in the dark whereas flow cytometry detects a weak signal.

The increased uptake of PI by S137-treated cells prompted us to investigate PS lipophilicity. Predicting logD for S137 and NMBN revealed that the former is about 1,500-fold more lipophilic than the latter at pH 7 (Fig. 10A). Indeed, S137 has a logD value comparable to that of ergosterol (Fig. 10B). These results indicate that S137 mainly accumulates at the cell membrane, potentially disturbing it and subsequently increasing PI permeability.

On the other hand, NMBN is only moderately lipophilic, which, combined with its positive charge, makes the PS a good candidate for mitochondria targeting (Rashid and Horobin 1990). Accordingly, the lipophilicity of NMBN is comparable to that of the

mitochondria-specific dye MitoTracker™ Red CMXRos (Fig. 10B). Use of the mitochondrial membrane potential indicator JC-1 revealed that NMBN caused considerable membrane depolarization already in the dark whereas S137 treatment was not different from untreated cells (Fig. 7). The fact that S137 is also a lipophilic cationic compound could indicate that it also targets mitochondria. However, extremely lipophilic compounds can take as long as hours or even days to diffuse through the lipid bilayer, a task that is achieved within minutes for moderately lipophilic molecules (Baláž 2000; Rashid and Horobin 1990). Therefore, under our experimental conditions in which cells and PS were allowed to interact for 30 min, the most likely outcome is that NMBN accumulates in mitochondria while S137, owing to its very high lipophilicity, is trapped at the cell membrane.

The reduced mitochondrial membrane potential observed after NMBN treatment could affect the outcome of some commonly used fluorescent dyes for monitoring reactive species production. This is the case for DHR-123. Oxidation of DHR-123 produces rhodamine-123 which localizes to mitochondria. However, rhodamine-123 accumulation is dependent on mitochondrial status: loss of membrane potential reduces dye accumulation and therefore washes away the fluorescent signal (Scaduto and Grotyohann 1999). In our experiments, rhodamine-123 signal was increased for S137 at 3 J cm^{-2} when compared to NMBN, which would be a plausible explanation for the higher mortality achieved by S137 (Fig. 8). However, this result needs to be interpreted with care. Because NMBN caused mitochondrial membrane depolarization already in the dark, then rhodamine-123 accumulation and signal could be hindered in NMBN-treated cells. In support of this hypothesis, rhodamine-123 fluorescence did not increase for either S137 or NMBN when fluence increased (Fig. 8), probably as a consequence of the reduced mitochondrial membrane potential at higher fluences (Fig. 7).

To overcome this limitation, we used DHE as a marker for the production of reactive species as it does not depend on mitochondrial status. The fact that NMBN and S137 produced approximately the same amount of reactive species at all light fluences tested (Fig. 9) indicates that it is most likely PS subcellular localization, and not the amount of reactive species generated, the deciding factor for APDT efficiency under our experimental conditions. In support of this hypothesis, prior work evaluating a series of photophysically similar porphyrin PS reported that photodynamic efficiency increases with increasing membrane binding and is only partially dependent on mitochondria localization (Pavani et al. 2009). Also, for PS targeting mitochondria, loss of membrane potential resulted in decreased binding (Pavani et al. 2009), a feature that could affect the outcome of APDT employing mitochondria-targeting PS such as NMBN.

5. Conclusion

Taken together, our results indicate that S137 and NMBN localize to different subcellular structures and hence inactivate *C. albicans* cells via different mechanisms. S137 localizes mostly to cell membrane and, upon light exposure, photo oxidizes membrane lipids, which in turn could change membrane permeability to S137 itself and allow the PS to reach other intracellular sites (Bocking et al. 2000). On the other hand, NMBN readily localizes to mitochondria and exerts its photodynamic effects there, which was observed to be a less effective way to achieve cell death at lower fluences. Finally, while using a combination of fluorescent dyes allowed us to better comprehend APDT with two distinct PS, the use of individual stains could be problematic: FUN-1 as a vital stain could not tell apart the differences in survival between S137 and NMBN at 3 J cm^{-2}, DHR-123 depends on mitochondrial status which was affected by NMBN in the dark; and DHE is only a general indicator of reactive species production and cannot take into

account that the same species could differently affect survival depending on where it is generated.

Acknowledgments

We thank Eduardo Tozatto and Fabiana Rossetto de Moraes, both from Faculdade de Ciências Farmacêuticas de Ribeirão Preto, for confocal microscopy and flow cytometry analyses, respectively. This work was supported by the State of São Paulo Research Foundation (FAPESP) grants 2012/15204-8 and 2016/11386 as well as by the National Council for Scientific and Technological Development (CNPq) grants 425998/2018-5 and 307738/2018-3 to G.UL.B. We sincerely thank FAPESP for a post-doc fellowship to G.B.R. (2012/22933-6) and for a Ph.D. scholarship to G.T.P.B. (2015/24305-0).

REFERENCES

Baláž, Š., 2000 Lipophilicity in trans-bilayer transport and subcellular pharmacokinetics. *Perspectives in Drug Discovery and Design* 19:157-177.

Basiji, D.A., W.E. Ortyn, L. Liang, V. Venkatachalam, and P. Morrissey, 2007 Cellular image analysis and imaging by flow cytometry. *Clin Lab Med* 27 (3):653-670, viii.

Bocking, T., K.D. Barrow, A.G. Netting, T.C. Chilcott, H.G. Coster *et al.*, 2000 Effects of singlet oxygen on membrane sterols in the yeast *Saccharomyces cerevisiae*. *Eur J Biochem* 267 (6):1607-1618.

Brancini, G.T., G.B. Rodrigues, M.S. Rambaldi, C. Izumi, A.P. Yatsuda *et al.*, 2016 The effects of photodynamic treatment with new methylene blue N on the *Candida albicans* proteome. *Photochem Photobiol Sci* 15 (12):1503-1513.

Castano, A.P., T.N. Demidova, and M.R. Hamblin, 2004 Mechanisms in photodynamic therapy: part one—-photosensitizers, photochemistry and cellular localization. *Photodiagnosis Photodyn Ther* 1 (4):279-293.

Chang, Z., V. Yadav, S.C. Lee, and J. Heitman, 2019 Epigenetic mechanisms of drug resistance in fungi. *Fungal Genet Biol* 132:103253.

Dai, T., V.J. Bil de Arce, G.P. Tegos, and M.R. Hamblin, 2011 Blue Dye and Red Light, a Dynamic Combination for Prophylaxis and Treatment of Cutaneous *Candida albicans* Infections in Mice. *Antimicrob Agents Chemother* 55 (12):5710-5717.

Davey, H.M., and P. Hexley, 2011 Red but not dead? Membranes of stressed *Saccharomyces cerevisiae* are permeable to propidium iodide. *Environ Microbiol* 13 (1):163-171.

de Menezes, H.D., A.C. Pereira, G.T.P. Brancini, H.C. de Leao, N.S. Massola Junior *et al.*, 2014 Furocoumarins and coumarins photoinactivate *Colletotrichum acutatum*

and *Aspergillus nidulans* fungi under solar radiation. *Journal of Photochemistry and Photobiology B-Biology* 131:74-83.

de Menezes, H.D., L. Tonani, L. Bachmann, M. Wainwright, G.U. Braga *et al.*, 2016 Photodynamic treatment with phenothiazinium photosensitizers kills both ungerminated and germinated microconidia of the pathogenic fungi *Fusarium oxysporum*, *Fusarium moniliforme* and *Fusarium solani*. *J Photochem Photobiol B* 164:1-12.

Gonzales, J.C., G.T.P. Brancini, G.B. Rodrigues, G.J. Silva-Junior, L. Bachmann *et al.*, 2017 Photodynamic inactivation of conidia of the fungus *Colletotrichum abscissum* on *Citrus sinensis* plants with methylene blue under solar radiation. *J Photochem Photobiol B* 176:54-61.

Köhler, J.R., A. Casadevall, and J. Perfect, 2015 The Spectrum of Fungi That Infects Humans. *Cold Spring Harb Perspect Med* 5 (1).

Limper, A.H., A. Adenis, T. Le, and T.S. Harrison, 2017 Fungal infections in HIV/AIDS. *Lancet Infect Dis* 17 (11):e334-e343.

Nishimoto, A.T., C. Sharma, and P.D. Rogers, 2020 Molecular and genetic basis of azole antifungal resistance in the opportunistic pathogenic fungus *Candida albicans*. *J Antimicrob Chemother* 75 (2):257-270.

Pavani, C., A.F. Uchoa, C.S. Oliveira, Y. Iamamoto, and M.S. Baptista, 2009 Effect of zinc insertion and hydrophobicity on the membrane interactions and PDT activity of porphyrin photosensitizers. *Photochem Photobiol Sci* 8 (2):233-240.

Perlin, D.S., R. Rautemaa-Richardson, and A. Alastruey-Izquierdo, 2017 The global problem of antifungal resistance: prevalence, mechanisms, and management. *Lancet Infect Dis* 17 (12):e383-e392.

Rashid, F., and R.W. Horobin, 1990 Interaction of molecular probes with living cells and tissues. Part 2. A structure-activity analysis of mitochondrial staining by cationic probes, and a discussion of the synergistic nature of image-based and biochemical approaches. *Histochemistry* 94 (3):303-308.

Rhodes, J., and M.C. Fisher, 2019 Global epidemiology of emerging *Candida auris*. *Curr Opin Microbiol* 52:84-89.

Rodrigues, G.B., M. Dias-Baruffi, N. Holman, M. Wainwright, and G.U. Braga, 2013 In vitro photodynamic inactivation of *Candida* species and mouse fibroblasts with phenothiazinium photosensitisers and red light. *Photodiagnosis Photodyn Ther* 10 (2):141-149.

Rodrigues, G.B., L.K. Ferreira, M. Wainwright, and G.U. Braga, 2012 Susceptibilities of the dermatophytes *Trichophyton mentagrophytes* and *T. rubrum* microconidia to photodynamic antimicrobial chemotherapy with novel phenothiazinium photosensitizers and red light. *J Photochem Photobiol B* 116:89-94.

Scaduto, R.C., and L.W. Grotyohann, 1999 Measurement of mitochondrial membrane potential using fluorescent rhodamine derivatives. *Biophys J* 76 (1 Pt 1):469-477.

Shor, E., and D.S. Perlin, 2015 Coping with Stress and the Emergence of Multidrug Resistance in Fungi. *PLoS Pathog* 11 (3).

Tonani, L., N.S. Morosini, H. Dantas de Menezes, M.E. Nadaletto Bonifacio da Silva, M. Wainwright *et al.*, 2018 In vitro susceptibilities of *Neoscytalidium* spp. sequence types to antifungal agents and antimicrobial photodynamic treatment with phenothiazinium photosensitizers. *Fungal Biol* 122 (6):436-448.

Wainwright, M., and R.M. Giddens, 2003 Phenothiazinium photosensitisers: choices in synthesis and application. *Dyes and Pigments* 57 (3):245-257.

Wainwright, M., T. Maisch, S. Nonell, K. Plaetzer, A. Almeida *et al.*, 2017 Photoantimicrobials-are we afraid of the light? *Lancet Infect Dis* 17 (2):e49-e55.

571 Wainwright, M., K. Meegan, and C. Loughran, 2011 Phenothiazinium photosensitisers
572 IX. Tetra- and pentacyclic derivatives as photoantimicrobial agents. *Dyes and*
573 *Pigments* 91 (1):1-5.